Discover Mechanical Engineering

Research

Flattening behaviour of weft-knitted spacer fabrics

Ulysse Le Coz[1] · Pierre Ringenbach[1] · Atsushi Sakuma[1] · Annie Yu[2]

Received: 10 July 2024 / Accepted: 4 November 2024
Published online: 13 November 2024

Abstract
Weft-knitted spacer fabrics are thick 3D knitted structures prized for their cushioning properties which have gathered increasing attention in the last decade. The thickness of a spacer fabric is one of its most influential parameters and strongly impacts its cushioning properties, wearability, thermal insulation or permeability. However, the fabric's natural undulation and high deformability make its thickness measurement uneasy. The current standard measurement methods require to measure the fabric thickness after compressing it until a fixed threshold stress value is reached to flatten it. The diversity of these threshold values is confusing, and each of them is unsuitable to variety of fabric rigidity. In this article, a standard for thickness evaluation was proposed and used to measure the thickness of 20 samples knitted with 5 independent parameters. The measured thickness was compared to the thickness measured at a threshold value of 1 kPa and to a theoretical thickness. The proposed measurement standard was proved reproducible and efficient for all fabrics when the threshold measures showed large errors on the softer and stiffer samples. The flattening stress of the fabrics ranged from 86 to 5262 Pa and could not be approximated by a single standard value. The theoretical thickness was more accurate, predicting the thickness with an average error of 3.8%.

Keywords Weft knitted spacer fabrics · Thickness measurement · Flattening · Compression · Model

List of symbols

C_l	Error coefficient of the linear model
C_s	Error coefficient of the standard method
E	Effective Young's modulus in compression of the fabric in the thickness direction
E_l	Young's modulus in compression of the fabric measured with the linear model
E_s	Young's modulus of the fabric measured with the standard method
e	Effective compression stiffness of the fabric in the thickness direction
e'	Effective compression stiffness of the spacer units in the thickness direction
F	Compression force of the fabric in the thickness direction
F_f	Flattening force of the fabric measured with the standard method
F_l	Flattening force of the fabric measured with the linear model
F_0	Compression force at the start of the standard analysis
G	Distance between the needles on the knitting machine needle bed
h	Maximum height of the fabric
L	Length of the spacer yarn between the tucks
n	Needle distance between the tucks

✉ Ulysse Le Coz, ulysse.lecoz@yahoo.fr | [1]Graduate School, Department of Advanced Fibro-Science, Kyoto Institute of Technology, Sakyo-Ku, Kyoto, Japan. [2]School of Fashion and Textiles, The Hong Kong Polytechnic University, Hong Kong, China.

S	Standard deviation of the fabric thickness normal distribution
W	Width of the outer layer's loops
T_{av}	Average thickness of the fabric
T_i	Ideal thickness of the fabric
T_l	Thickness of the fabric measured with the linear model
T_m	Thickness of the fabric on the knitting machine
T_t	Thickness of the fabric at a threshold stress value
T_s	Thickness of the fabric measured with the standard method
T_0	Thickness of the fabric at the start of the standard analysis
δ	Displacement of the compression platen
δ_{av}	Displacement at the average thickness of the fabric
δ_c	Displacement at the initial contact between the platen and the fabric
δ_f	Displacement at the thickness measured with the standard method
δ_l	Displacement at the thickness measured with the linear model
δ_{max}	Initial distance between the compression platen and the support
δ_t	Displacement at the thickness measured at a threshold stress value
δ_0	Displacement at the start of the standard analysis
ε	Compression strain of the fabric in the thickness direction
ϕ	Probability density function of the thickness distribution
Φ	Cumulative distribution function of the thickness distribution
σ	Compression stress of the fabric in the thickness direction
σ_f	Flattening stress of the fabric measured with the standard method
σ_l	Flattening stress of the fabric measured with the linear model

1 Introduction

Spacer fabrics are 3D knitted structures showing high thickness, they can be knitted using warp-knitting or weft-knitting [1]. Despite the thickness being the major characteristic of this kind of fabric, until now, no method existed to rigorously measure it. This study is proposing a reproducible, rigorous and precise method to measure the thickness of such fabrics with a high precision.

Spacer fabrics may have different usages, such as thermal insulators [2, 3], thermoelectric generators [4–6], triboelectric generators [7], wearable sensors [8], sound absorption devices [9], medical devices [10], and others. However, they are mostly used for their spring-like compression behaviour which gives them very interesting cushioning [11–16] and vibration absorption [17–22] properties.

Therefore, the compression behaviour in its thickness direction is the most studied aspect of spacer knitted structures. Measuring the fabric thickness is necessary to its compression behaviour characterization for two reasons: calculating the fabric compression strain and removing the initial flattening force from the compression data. The fabric thickness is also a major parameter for most of its properties [23]. Although spacer fabrics can be described as flat, in reality the fabrics actually exhibit an irregular thickness and a slightly wavy shape (Fig. 1). Due to this, measuring precisely the thickness of spacer fabrics is an uneasy task and no satisfactory method is currently available. Given the waviness of spacer fabrics, measuring their thickness requires flattening them by compressing them in the thickness direction. But distinguishing the flattening of a spacer fabric from an actual compression is complex, previously no theory existed to determine exactly when a spacer fabric was flattened. Most studies measure the thickness of spacer fabrics after pressing them at fixed threshold stress values, those methods produce unprecise measure results which cannot be compared with each over.

Characterising the mechanical behaviour of textile sandwich structures is a complex matter as such materials have complex geometries and a great number of parameters, which make difficult to predict their behaviour [24].

The present study presents a standardised method to measure accurately the thickness and Young's modulus in compression of spacer fabrics through a compression test and a simple data processing. This method is compared with a simpler but less precise method relying on a linear model.

The 1 kPa threshold standard is investigated and the thickness measured using this method is compared with the more accurate measurement given by the newly developed standard.

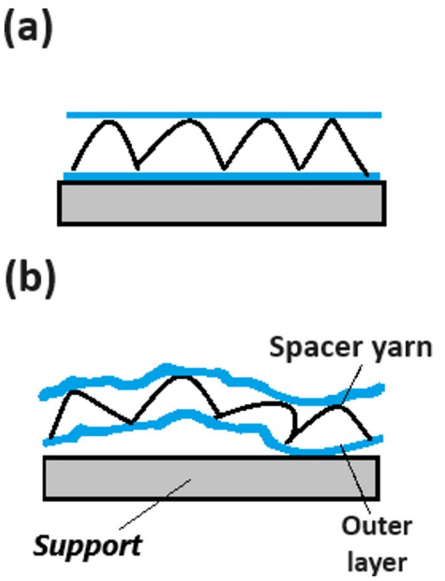

Fig. 1 (**a**) Ideal and (**b**) real shape of a spacer fabric

A simple geometric model has already shown good predictions of the thickness of spacer fabrics [1]. The efficiency of this model is investigated and compared with the more accurate measurement given by the newly developed standard.

This study is pursuing two aims: the measure of the spacer fabric thickness and the characterisation of the spacer fabric flattening behaviour. The proposed method aims to harmonise the confusing variety of existing methods and enable accurate measurements for all kinds of spacer fabrics. The study also proposes a mathematical model of the flattening behaviour which aims to predict efficiently the stress required to flatten a spacer fabric.

2 Materials and methods

2.1 Materials

Weft-knitted spacer fabrics are composed of three distinct parts (Fig. 2a): two flat jersey knitted outer layers (Fig. 2b) separated by a spacer layer (Fig. 2c). During the fabrics knitting on a double needle bed weft-knitting machine, a stiff spacer yarn alternatively tucks the two outer layers to connect them (Fig. 3). The outer layers being knitted with elastic yarns, they contract after the knitting. To keep its length the spacer yarn between two tucks pushes the two outer layers away from each over, thickening the fabric. When the fabric is compressed the spacer yarn bends to act as a spring between the outer layers.

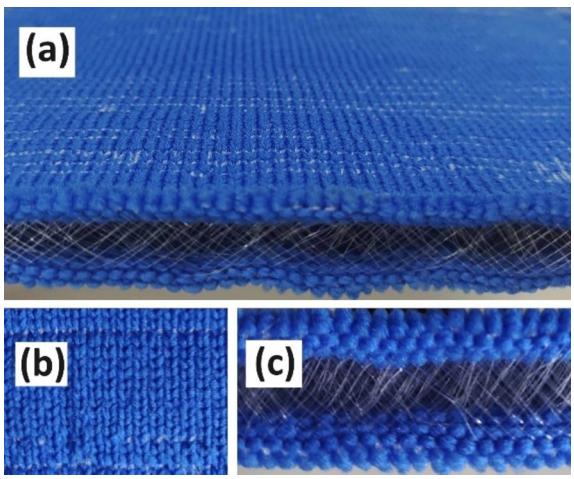

Fig. 2 A weft-knitted spacer fabric (**a**), its outer layer in top view (**b**) and spacer layer in warp view (**c**)

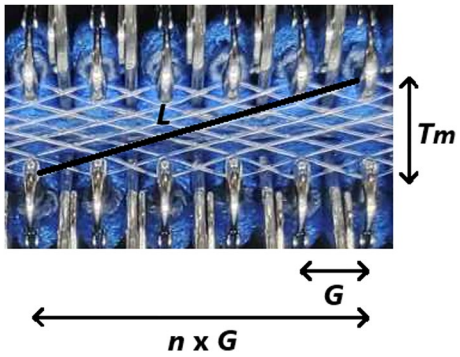

Fig. 3 Spacer layer on the knitting machine

The knitting structure of a weft-knitted spacer fabric is defined by its needle distance *n*, which represents the number of needles horizontally separating two adjacent tucks (Fig. 3). The spacer yarn tucks alternatively the two outer layers each n loops, it then tucks the same row of one outer layer at one loop every 2n loops. For a stable knitting, each loop of the outer layer can accommodate only one tuck of the spacer yarn (Fig. 4). In total, 2*n* different spacer yarns are required to tuck all the loops on a same row of the outer layer, for each row of the outer layer the spacer layer has 2*n* rows. To investigate the impact of the needle distances, the samples were knitted with three different needle distances: $n = 3$, 5, and 7.

A total of 20 weft-knitted spacer fabric samples was produced on a 10-gauge double-bed weft-knitting machine of the grade "SWG 091N2" (Shima Seiki MFG. LTD.; Wakayama, Japan) using three components: an outer-layer yarn, an elastic yarn added to the outer-layer yarn and a polymer monofilament for the spacer yarn (Table 1). On this 10-gauge machine the needles of a same needle bed are separated by a needle gap $G = 2.54$ mm and the fabrics all have a machine thickness $T_m = 3.5$ mm (Fig. 3).

The outer layer was knitted with two different yarns: a polyethylene terephthalate (PET) drawn textured yarn of the grade "Amossa LS1/20" (Assist Ltd; Osaka, Japan) and a spun yarn of the grade "Dralon cotton Ne32/1" (Katamosa Co. Ltd; Ginan, Japan) composed of 50% cotton and 50% acrylic. The cotton-acrylic yarn is very stiff, whereas the PET yarn shows a high elastic elongation which tends to increase the contraction of the spacer fabric after the knitting (Fig. 5).

Two core-spun elastic yarns of different linear densities were added to the outer layer yarn during the knitting process to increase the shrinkage of the fabrics (Tables 1 and 2, Fig. 6). Three Polyamide-6 (PA6) and one PET stiff monofilaments of different diameters were used as spacer yarns (Tables 1 and 2).

The characterisation of the yarns was done through tensile tests conducted on a benchtop universal testing machine. The outer layer yarns and the elastic yarns were tested using respectively 3 and 5 specimens of 100 mm length on a machine of the grade "EZ-LX 500N" (Shimadzu Corporation; Kyoto, Japan) whereas the spacer yarns were tested using 10 specimens of 150 mm length on a machine of the grade "EZ-S 500N" (Shimadzu Corporation; Kyoto, Japan). All the tests were performed at a speed of 1 $mm.s^{-1}$.

The weft-knitted samples were produced with a width of 98 loops (248.92 mm on the machine) and a length of 350 loops. All the samples produced and tested are summarized in the Table 2. Each sample was knitted with respective

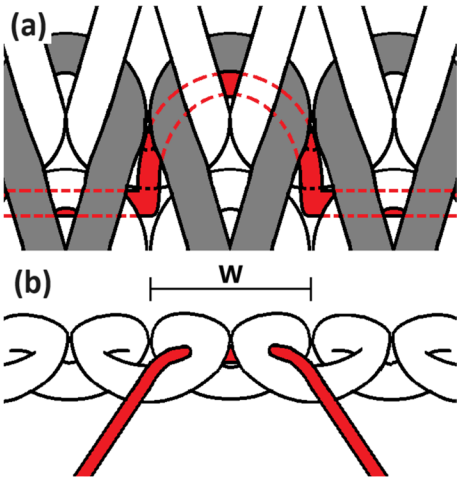

Fig. 4 Spacer yarn (red) tucking a loop of the outer layer (white and grey) in (**a**) top view and (**b**) warp view

Table 1 Yarns properties

Product name	Function	Material	Diameter (mm)	Linear density (Tex)	Elastic modulus (cN)	Tenacity (cN/Tex)
Amossa LS1/20	Outer layer yarn	PET	/	50	2970 ± 738	39.86 ± 0.62
Dralon-Cotton Ne32/1		Cotton 50% -acrylic 50%			4797 ± 1818	13.23 ± 1.01
Marulon ST6800	Elastic yarn	Spandex	/	39	49.0 ± 5.9	6.58 ± 0.99
Marulon S1470				15	14.7 ± 2.2	10.52 ± 1.97
PA8	Spacer yarn	PA 6	0.08	5.4	1760 ± 554	/
PA12			0.12	12.3	3859 ± 475	
PA14			0.14	16.7	5101 ± 567	
PE8		PET	0.08	6.9	4158 ± 618	

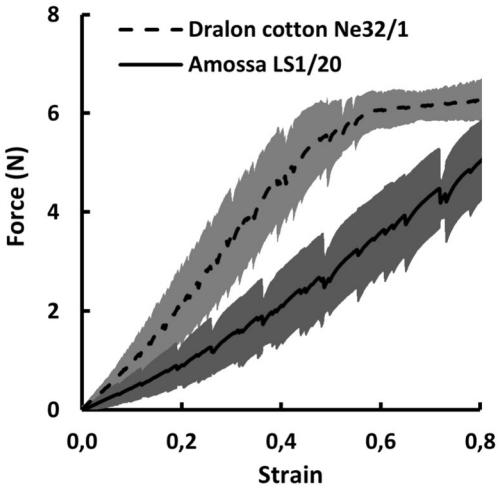

Fig. 5 Average value (black) and standard-deviation (grey) of the tensile force of the two outer layer yarns in function of the strain

stitch values of 70 and 0 for the outer layer and the spacer layer, except for the A12N3S S10 sample, which was knitted with a stitch value of 10 for the spacer yarn. The 20 samples were defined by 5 independent parameters: the knitting structure, the outer layer yarn, the elastic yarn, the spacer yarn diameter and the spacer yarn material. All the samples were submitted to a compression test and the obtained data was processed to identify their thickness, flattening properties and compression properties.

A warp-knitted spacer fabric with its spacer layer made entirely with a Polyethylene (PE) monofilament of diameter 0.07mm was also investigated in this study.

2.2 Methods

A spacer fabric compressed in its thickness direction between two flat compression platens initially at a distance δ_{max} shows a compression behaviour following four steps [11, 14, 25, 26] (Fig. 7):

Step I: Flattening

Initially the outer layers of the fabric are not perfectly planar, and the thickness is irregular (Fig. 1b). During this stage, the compression platens is flattening the fabric.

Table 2 Weft-knitted pacer fabric samples properties

Outer layer Yarn	Spacer yarn material	Spacer yarn diameter (mm)	Needle distance	Elastic yarn	Sample name
Dralon-Cotton Ne32/1	PA 6	0.12	5	Marulon ST6800	DA12N5ST
			7		DA12N7ST
Amossa LS1/20		0.08	5		A8N5ST
		0.12			A12N5ST
		0.14			A14N5ST
		0.08	7		A8N7ST
		0.12			A12N7ST
		0.14			A14N7ST
		0.08	3	Marulon S1470	A8N3S
		0.12			A12N3S
		0.12			A12N3S S10
		0.14			A14N3S
		0.08	5		A8N5S
		0.12			A12N5S
		0.14			A14N5S
		0.08	7		A8N7S
		0.12			A12N7S
		0.14			A14N7S
	PET	0.08	3		E8N3S
			5		E8N5S

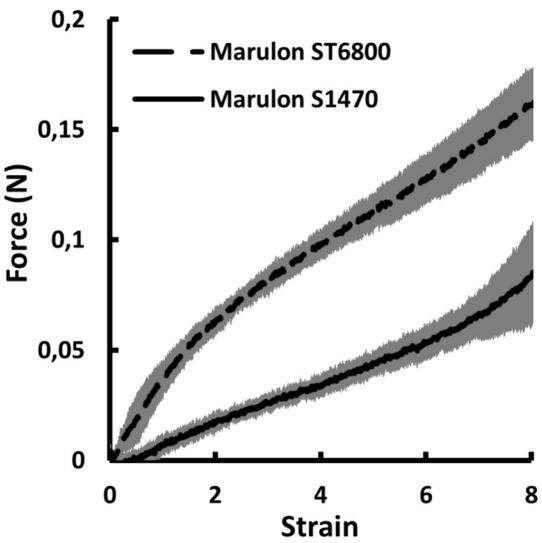

Fig. 6 Average value (black) and standard-deviation (grey) of the tensile force of the two elastic yarns in function of the strain

Step II**:** Linear compression

Once the fabric is flattened and the outer layers are planar and parallel (Fig. 1a), the spacer yarn inside the fabric bends, resulting in a linear compression behaviour.

Step III**:** Plateau

As the spacer yarn bends excessively, it can no longer provide vertical resistance, leading to a plateau in the compression behaviour.

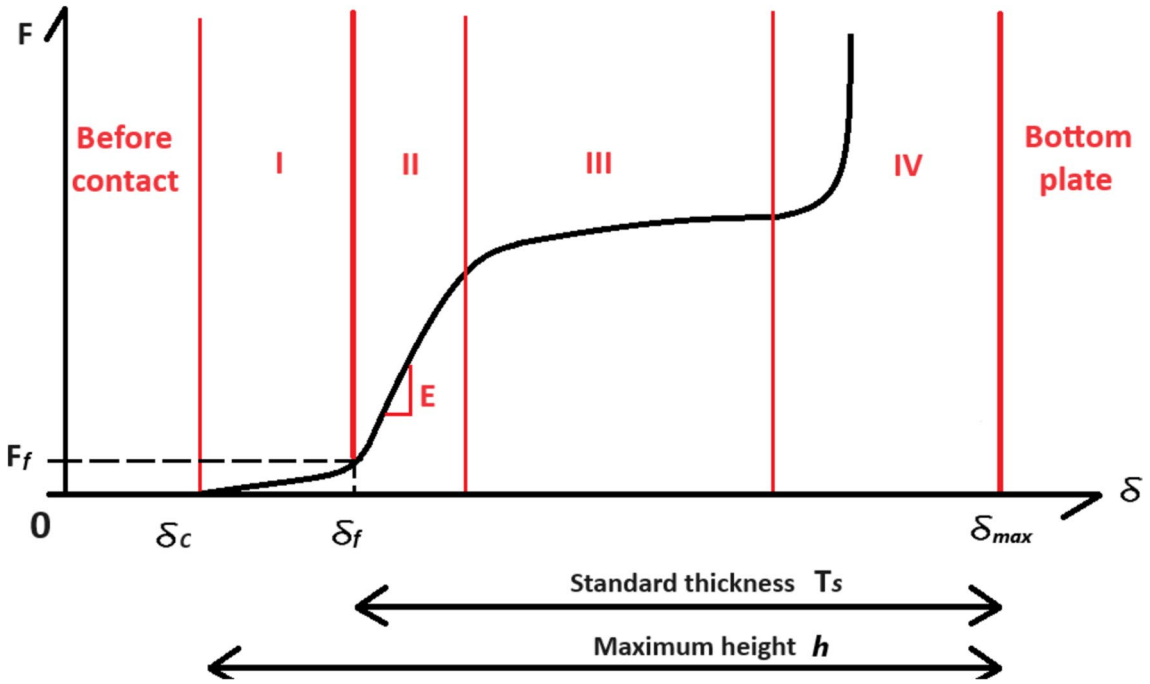

Fig. 7 Compression behaviour of the spacer fabrics

Step IV**:** Densification

Finally, the spacer yarn is fully bent, the fabric has lost its thickness, and the two outer layers touch each other. The spacer fabric compression becomes the compression of its two flat knitted outer layers.

The fabric thickness cannot be measured at δ_c when the compression platen starts to touch the top of the fabric, this method is measuring the maximal height of the fabric and would overestimate its effective thickness (Fig. 7). The fabric is still waved in its early compression and is fully flattened only when it enters a linear compression behaviour. Therefore, the proposed standard thickness T_s is set as the thickness of the spacer fabric when pressed until a linear compression behaviour at δ_f, and $T_s = \delta_{max} — \delta_f$.

The flattening (step I) has little impact on the compression stress because the flattening force F_f tends to be low, but the measure of the flattening displacement δ_f is necessary to determine the standard thickness of the fabric.

Because the precise stress required to flatten the fabric is unknown prior to the compression, the thickness of spacer fabrics is often measured under a fixed threshold stress value. Using a standardized measurement method with a threshold stress value has two primary advantages: it is a quick process which does not require extensive data processing, and it ensures reproducibility. However, this method can give significantly different measurements for fabrics of similar thickness but different rigidity. Fabrics made of harder materials will reach the threshold stress value more rapidly than those made of softer materials, leading to inaccurate measures (Fig. 8).

Because no standard threshold stress value has been defined specifically for 3D knitted spacer fabrics, their thickness is currently measured with standard methods designed for flat knitted fabrics or without following any standard at all. The European standard EN ISO 5084 [27] and the Japanese standard JIS L 1096 [28] set a threshold stress value of 1 kPa. This ISO standard method was used by several searchers to measure the thickness of weft-knitted spacer fabrics [2, 22, 29]. Yu et al. [17] used the 1 kPa threshold stress value without mentioning the ISO or JIS standards. The ISO standard also proposes the use of a stress value of 0.1 kPa for certain knitted fabrics without precising if spacer fabrics are concerned, this alternative standard was also used with weft knitted spacer fabrics [3, 30]. Yu et al. [18] measured the thickness of weft-knitted spacer fabrics following the ISO standard method but used a 0.5 kPa threshold stress value.

Rajan et al. [12, 31] and Li et al. [15, 16] used the ASTM D1777 – 96 standard measurement method [32] with respective stress values of 100gf/cm^2 and 4gf/cm^2 (respectively 9.81 kPa and 0.39 kPa). Liu et al. [9, 33] measured the thickness of weft-knitted spacer fabrics using the Kawabata Evaluation System (KES) [34] with a threshold stress value of 0.5gf/mm (49 Pa) [35]. Chen et al. [36] used a threshold stress value of 50 Pa without mentioning any standard method. This diversity is creating confusion for the searchers who are discussing spacer fabric's properties with different conceptions

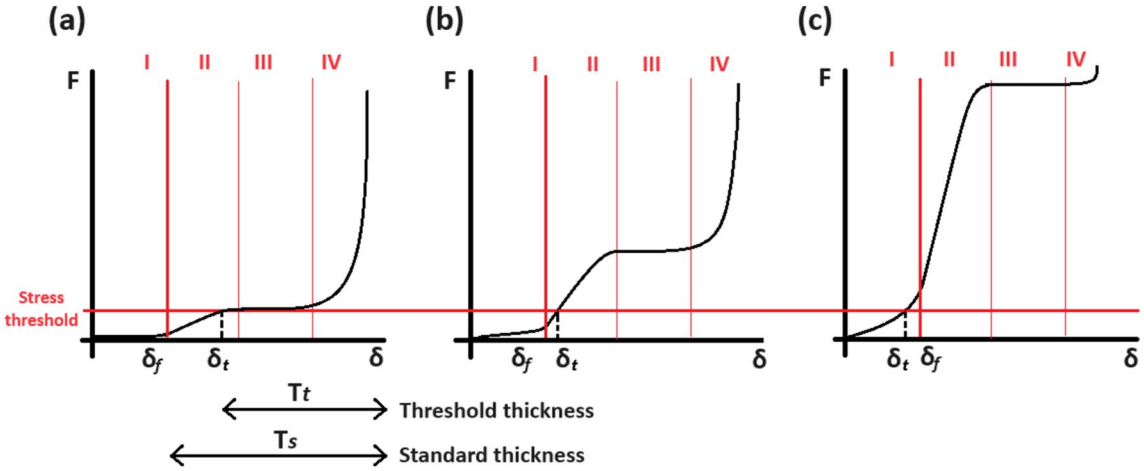

Fig. 8 threshold and standard thickness measurements for fabrics of similar thickness with (**a**) low, (**b**) medium and (**c**) high rigidities

of the fabric thickness. The new standard thickness measurement method is proposed to harmonize the definition of the spacer fabric thickness without the errors induced by an arbitrary threshold.

Because the stress required to flatten the samples cannot be predicted, they have to be subjected to a full compression test in their thickness direction. This test indicates the thickness, the flattening behaviour and the compression behaviour of the samples. The compression is performed by a compression platen with a circular section of 116 mm diameter on a benchtop universal testing machine of the grade "EZ-S 500N" (Shimadzu Corporation; Kyoto, Japan). The samples were laid flat on a metal plate attached to the lower supporter of the machine before being pressed at three distinct spots at a speed of 0.1 mm/s. The test was conducted from an initial distance between the compression plate and the support of $\delta_{max} = 16$ mm until a 200N resistance was reached (Fig. 9). The warp-knitted samples and some weft-knitted samples were compressed until 250 or 300N to ensure that the densification stage was attained.

The samples were not cut in smaller specimens to prevent the deformation of the outer layer. Cutting the fabric causes the outer layer to strongly contract near the cut, the cut outer layer then rolls up and makes the fabric thicker on its edges (Fig. 10). The difference of contraction between the middle of a cut fabric and its edges also increases the waving.

Fig. 9 Compression test setup

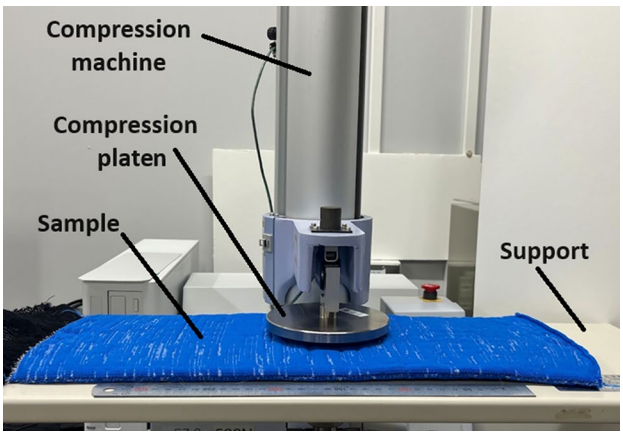

Fig. 10 Compression of (**a**) uncut and (**b**) cut samples

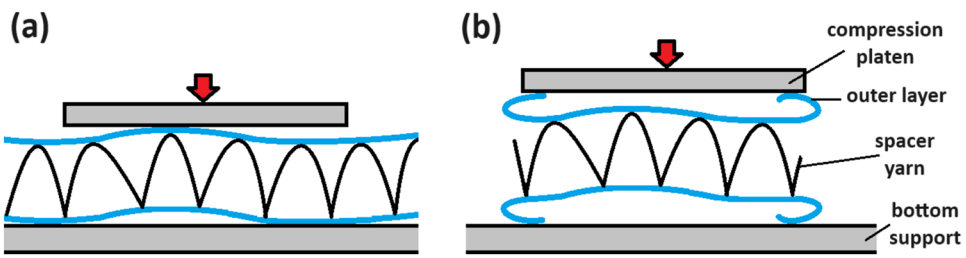

The thickness of weft-knitted spacer fabrics can also be estimated without compression test by using the knitting machine's dimensions. Because the spacer yarn is straight between the tucks on the knitting machine, its length between two tucks L can be calculated using the length of the gap between two needles G, the number of needles between the tucks n and the thickness on the machine T_m (Eq. 1) (Fig. 3). After the knitting process the spacer fabric falls from the machine and its outer layer shrinks so that the horizontal distance between two tucks is no longer n times G but n times the width of the loops W (Figs. 4 and 11). By considering that the spacer yarn remains straight after the shrinkage the ideal thickness T_i of the spacer layer can be calculated using the Eq. 2 (Figs. 11)

$$L = \sqrt{T_m{}^2 + (n \times G)^2} \tag{1}$$

$$T_i = \sqrt{L^2 - (n \times W)^2} \tag{2}$$

3 Results and discussion

3.1 New standard model

The section of a spacer yarn between two following tucks is called a spacer unit (Fig. 11), the entire spacer layer of a fabric can be assimilated to a repetition of this unit in the warp and weft directions (Fig. 12a). The total number of spacer units compressed during a compression test is noted N_u. By considering the different spacer units to behave like independent springs (Fig. 12b), the total compression force of the fabric can then be determined as the sum of the compression forces of all its spacer units (Fig. 12c). The units of a same fabric show different thickness, their distribution can be expected to follow a normal law $N(T_{av}, S^2)$ having for expectation T_{av} the average thickness of the spacer units and a variance S^2. The displacement of the compression platen when exactly half of the spacer units are already compressed is called $\delta_{av} = \delta_{max} - T_{av}$. After expressing the probability density function of the thickness distribution ϕ in function of the displacement δ (Eq. 3) and integrating it, the cumulative distribution function $\Phi(\delta)$ (Eq. 4) gives the proportion of spacer units having already started their compression at a given displacement (Fig. 13a). After considering that all the spacer units have the same compression stiffness e', the total compression stiffness of the fabric $e = e' \times N_u$ can be obtained using the Eq. 5 (Fig. 13b).

$$\phi(\delta) = \frac{1}{\sqrt{2\pi S^2}} e^{-\frac{(\delta - \delta_{av})^2}{2S^2}} \tag{3}$$

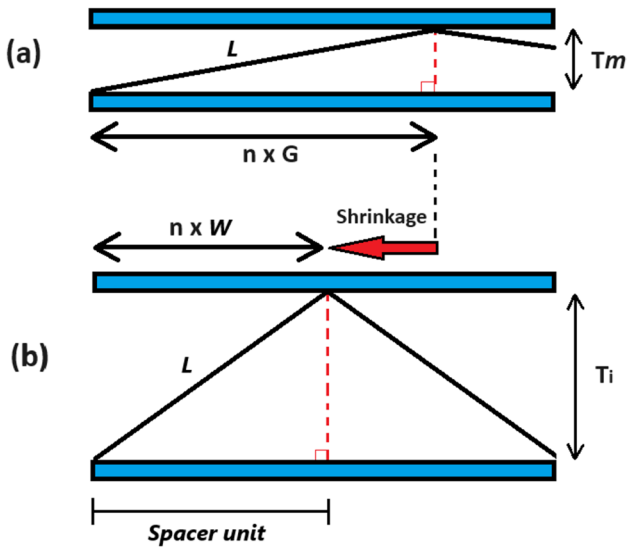

Fig. 11 Spacer fabric ideal dimensions (**a**) on machine and (**b**) after its shrinkage

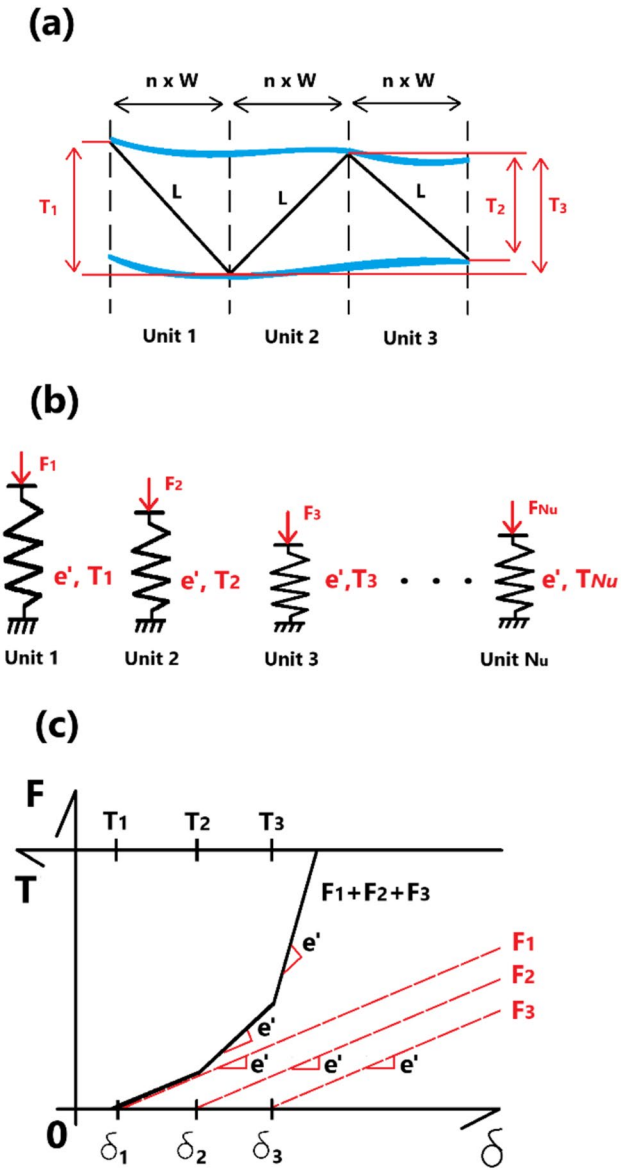

Fig. 12 Spacer units (**a**) geometry (**b**) spring-like characteristics (**c**) compression behaviour

$$\Phi(\delta) = \int_{-\infty}^{\delta} \phi(t)dt \tag{4}$$

$$\frac{dF(\delta)}{d\delta} = \Phi(\delta) \times e \tag{5}$$

The fabric is considered flattened when the compression platen reaches $\delta_f = \delta_{av} + S$, at this point already 84% of the spacer units are already in compression and the fabric can be considered to have a linear compression behaviour (Fig. 13a, c). The distance between the compression platen and the support gives the standard thickness of the fabric $T_s = \delta_m - \delta_f$.

The experimental value of the compression stiffness of the fabric can also be calculated from the experimental data using the least squares method (Eq. 6). The experimental stiffness of the fabrics first behaves like the cumulative distribution

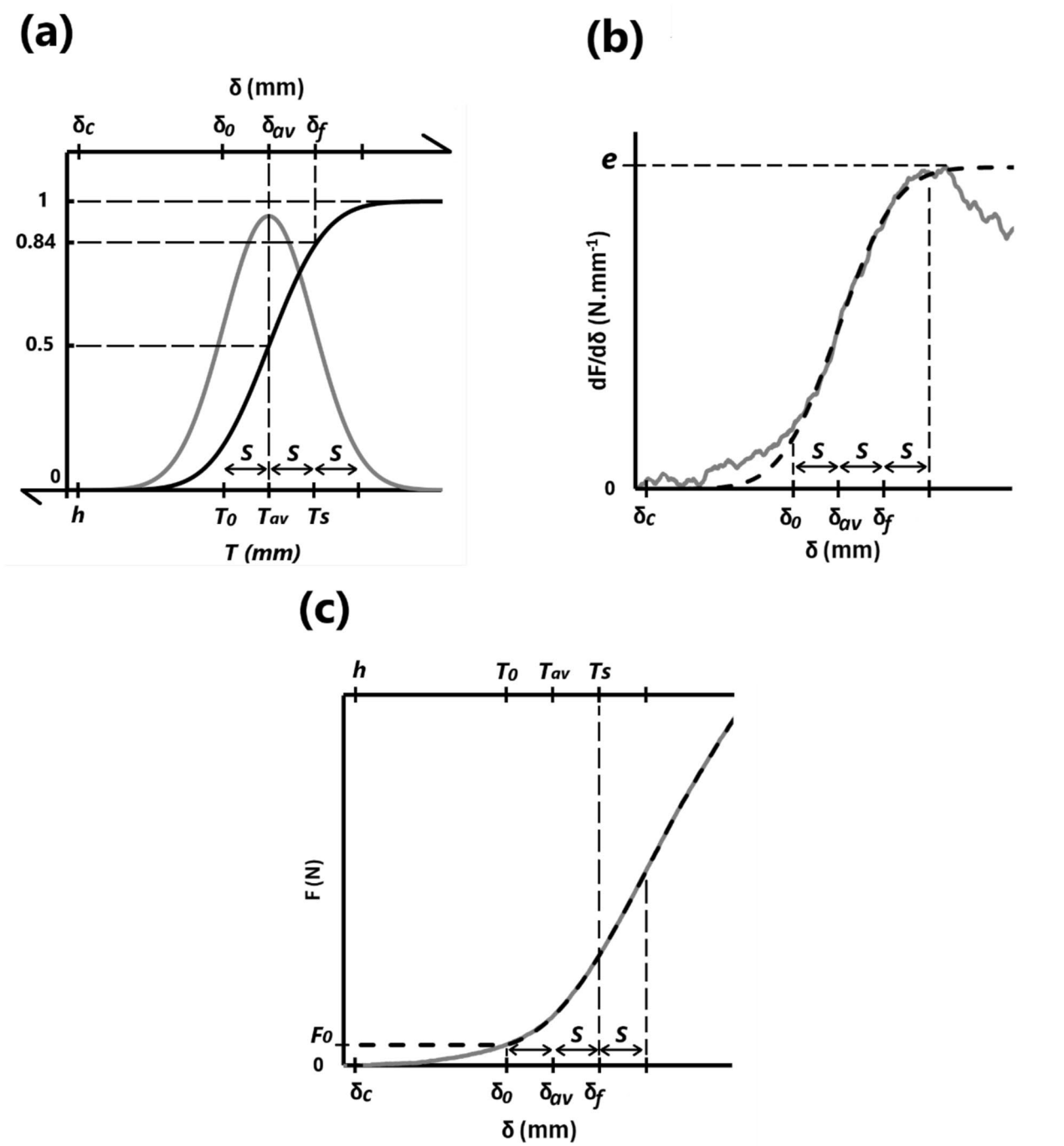

Fig. 13 Normal distribution of the thickness (grey) and proportion of compressed units (black) of the specimen 8AN7ST_1 (**a**), experimental (grey) and model (black) compression stiffness of the specimen 8AN7ST_1 (**b**) experimental (grey) and model (black) compression force of the specimen 8AN7ST_1 (**c**)

function of a normal law until a local maximum and then go down as the compression start to enter its plateau phase (step III). This local maximum is considered to be *e* the stiffness of the spacer units (Fig. 13b).

$$\frac{dF}{d\delta}(\delta_i) = \frac{N \times \sum_{-N/2<j<N/2} F(\delta_{i+j}) \times \delta_{i+j} - \left[\sum_{-N/2<j<N/2} F(\delta_{i+j})\right] \times \left[\sum_{-N/2<j<N/2} \delta_{i+j}\right]}{N \times \sum_{-N/2<j<N/2} (\delta_{i+j})^2 - \left[\sum_{-N/2<j<N/2} \delta_{i+j}\right]^2} \tag{6}$$

The force–displacement raw data were processed using a mathematical inverse analysis procedures and a function of the MS-Excel solver [37]. The analysis is a procedure used to determine the standard thickness T_s and the standard deviation S. The analysis is conducted around δ_{av}, it starts at $\delta_{av} - S = \delta_0$ and finishes at $\delta_{av} + 2S$. The analysis cannot start too far away from δ_{av} because the initial stiffness of the fabric is often caused by its waviness rather than the compression of the thickest spacer units (Fig. 13b). The analysis is setting the values of the two variables T_{av} and S, the parameter δ_{max} is set manually, the parameters δ_0, δ_{av}, e and T_s are automatically calculated by the Excell sheet. An error coefficient C_s is calculated by summing the square of the difference between the measured and calculated stress values for the same δ (Eq. 7). The analysis sets the optimal combination of variable values for S *and* T_{av} to reach the minimum value of the error coefficient C_s. After the solver determined the parameters T_s and S, the compression force $F(\delta)$ can be calculated from δ_0 by adding the integral of the model stiffness between δ_0 and δ to F_0 the force at δ_0 (Eq. 8) (Fig. 13c).

$$C_s(\delta_0, S, F, F_0, \Phi) = \sum_{\delta_0<\delta<\delta_0+2S} \left[\frac{dF(\delta)}{d\delta} - F_0 - \int_{\delta_0}^{\delta} \Phi(t) \times edt\right]^2 \tag{7}$$

$$F(\delta) = F_0 + \int_{\delta_0}^{\delta} \Phi(t) \times edt \tag{8}$$

The effective Young's modulus in compression E of the fabric is then calculated using the average value of the compression stiffness between δ_f and $\varepsilon(\delta_f + T_s / 10) = 10\%$ (Eq. 9).

$$E = \frac{T_s}{A} \times \left(\frac{\overline{dF}}{d\delta}\right)_{0<\varepsilon<10\%} \tag{9}$$

3.2 Linear model

A second analysis is conducted to determine the Young's modulus and thickness of the fabric using a linear model, the Young's modulus and thickness measured using this linear model are respectively noted E_l and $T_l = \delta_{max} - \delta_l$ (Eq. 10 and 11).

$$\sigma(\varepsilon) = E_l \times \varepsilon + \sigma_l \tag{10}$$

$$\varepsilon = \frac{\delta - \delta_l}{T_l} \tag{11}$$

The analysis compares the model stress value with the experimental value for ε between $\varepsilon(\delta_l) = 0\%$ and 10% (Fig. 14). The solver is setting the values of the three variables E_l, δ_l and σ_l, the parameter δ_{max} is set manually, the parameters T_l

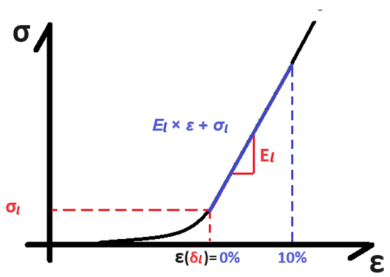

Fig. 14 Analysis process of the linear compression with the measured data (black), the calculated data (dark blue) and the variables set by the analysis (light red)

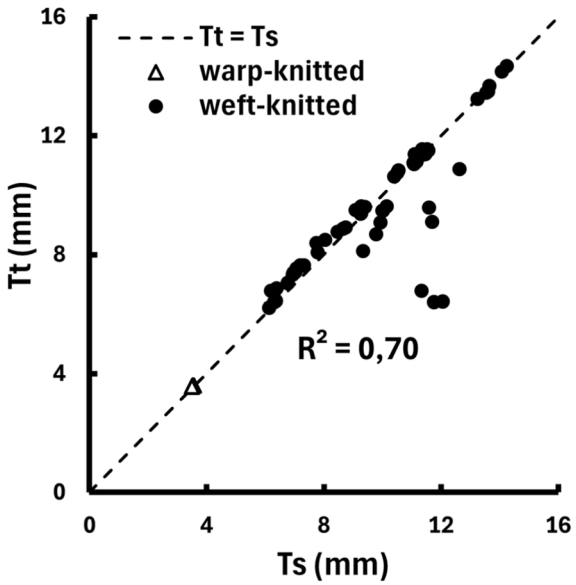

Fig. 15 Threshold thickness in function of the standard

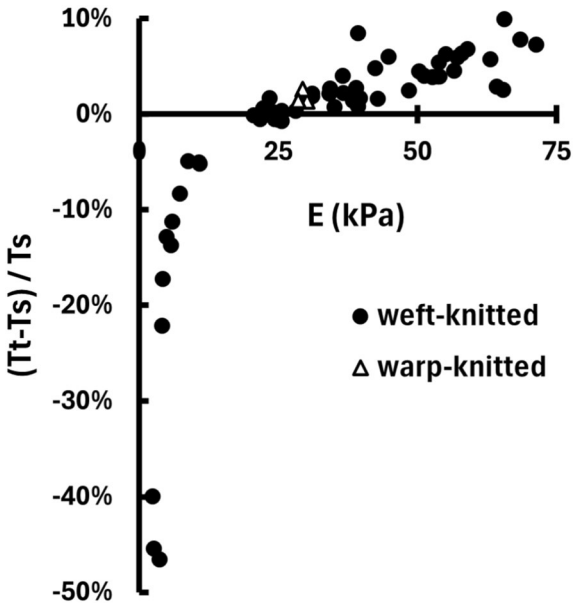

Fig. 16 Threshold thickness error in function of the Young's thickness of the specimens modulus of the specimens

and ε are automatically calculated by the Excell sheet. An error coefficient C_l is calculated by summing the square of the difference between the measured and calculated stress values for the same ε (Eq. 12). An optimal combination of variable values E, δ_l and σ_l is set to reach the minimum value of C_l.

$$C_l = \sum_{\varepsilon<10\%} [\sigma(\varepsilon) - E_l \times \varepsilon - \sigma_l]^2 \tag{12}$$

This second method is less precise than the first one and provide less information about the fabric thickness but is much simpler.

3.3 Efficiency of the 1 kPa threshold method

The thickness *Tt* of the samples is measured at the threshold stress value of 1 kPa, it often closely approximates the effective thickness for the tested samples (Figs. 15 and 16). Specifically, 41 out of 63 specimens exhibit less than a

5% difference from the standard thickness T_s. As expected, the softer and harder fabrics respectively need lower and higher threshold values. This standard seems effective enough for spacers with a Young's modulus in compression ranging between 20 and 50 kPa, but it appears completely inadequate for spacers with a Young's modulus in compression below 10 kPa (Fig. 16). The flattening stress of the samples ranges from 86 to 5262 Pa, suggesting that 1 kPa is generally a more suitable threshold than 0.1 or 10 kPa for fabrics of this kind. The warp-knitted samples show a very small variation between T_s and T_t, with an average value of 1.8%.

3.4 Efficiency of the geometric model

The ideal thickness T_i matches the standard thickness efficiently (Fig. 17), the absolute value of the variation of the ideal thickness from the standard thickness exhibits an average of 3.8% and a maximum of 9.5%. This model provides a more precise value of the thickness than the threshold method without requiring any compression test or data processing. Interestingly, this variation does not appear to be correlated with any of the fabric's properties. The ideal thickness should be larger than the standard thickness as it neglects the outer layer thickness covering the spacer layer (Fig. 4). In reality the spacer yarn doesn't remain straight between the two outer layers, it bends a little reducing the fabric thickness. For T_i to match T_s so accurately it appears that the thickness of the outer layer covering the spacer layer and the fabric thickness lost due to the spacer yarn bending are balancing each over. A better estimation of the outer layer thickness could allow to determine the average bending of the spacer layer of a fabric.

3.5 Efficiency of the linear model

The linear model gives very accurate values of the thickness for the fabrics with a needle distance n of 5 or 7, on the other hand most of the specimen with a needle distance $n = 3$ show variation between T_s and T_l above 6% (Fig. 18). For the Young's modulus, the linear model matches the standard method with less accuracy (Fig. 19). Once again, the samples with $n = 3$ show larger variation between E and E_l, almost half of the specimens having above 10% variation.

It is clear that the two models can produce different values from a same experiment and that they should not be considered as equivalent. The linear model tends to overestimate the thickness to calculate the error coefficient C_l on smaller δ values where F is also lower. Using the linear model to measure the thickness leads to unprecise values and should be avoided. On the other hand, the linear model focus on measuring the Young's modulus, its measure could be more accurate that the one given by the standard method. Measuring the elasticity through the linear model with a thickness T_s measured with the standard method might be the most rigorous way to proceed.

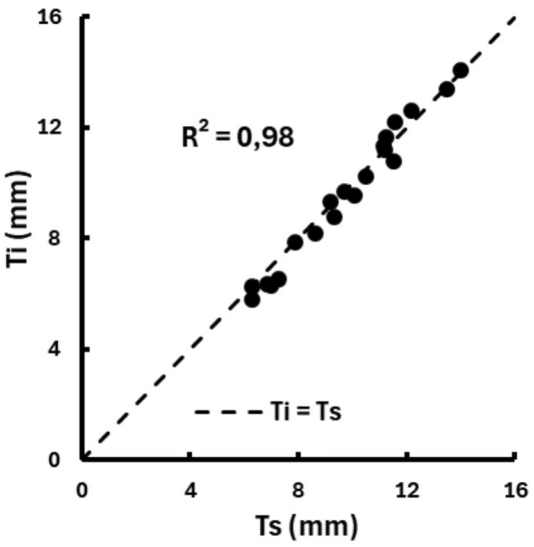

Fig. 17 Ideal thickness of the weft-knitted spacer fabrics in function of their standard thickness

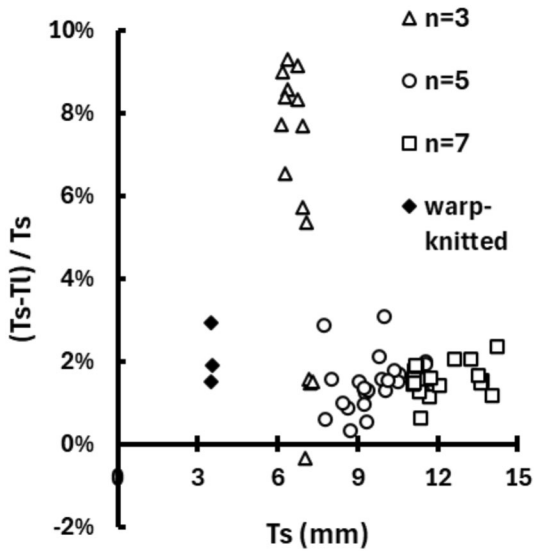

Fig. 18 Thickness error of the linear model in function

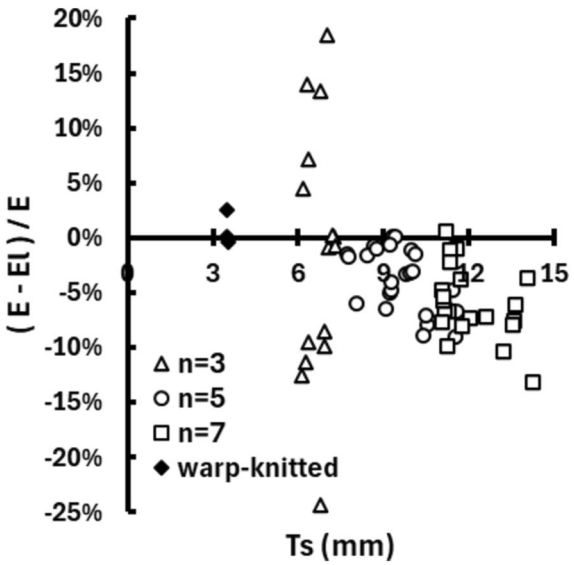

Fig. 19 Young's modulus error of the linear model in functionof the standard thickness of the specimens of the standard thickness of the specimens

3.6 Efficiency of the standard model

The model could match the experimental data very accurately, the analysis result shows a coefficient of determination with the experimental data of an average value $R^2 = 0.99990$. The flattening behaviour of the warp-knitted spacer sample too was modelized very precisely, the model and the experiment data having an average coefficient $R^2 = 0.99997$. The standard model can be widely used to efficiently measure the thickness of warp-knitted and weft-knitted fabrics by both the academic and industrial fields. Future models predicting the linear compression behaviour of spacer fabrics could also be enhanced by the use of the model presented in this study.

The standard deviation *S* of the thickness distribution is stable for the weft-knitted samples, showing an average value of 0.362 mm and a standard deviation of 0.055 mm. The value of S shows no correlation with the other properties of the fabrics, it might be linked to characteristics of the knitting machine. The flattening behaviour appears to be the same for all the weft-knitted spacer fabrics. The warp-knitted sample had smaller *S* values at 0.149 ± 0.017 mm, none of the weft-knitted samples has such a quick flattening.

The weft-knitted samples exhibit a linear relationship between their flattening force F_f and their stiffness *e* independently of the fabric parameters (Figs. 20 and 21). The ratio e / F_f remains stable, with an average value of 2.48 mm^{-1} and a standard deviation of 0.49 mm^{-1}.

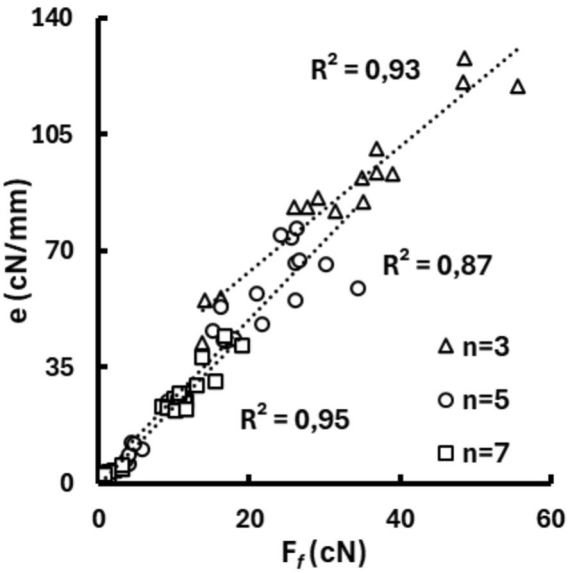

Fig. 20 Stiffness *e* in function of the flattening

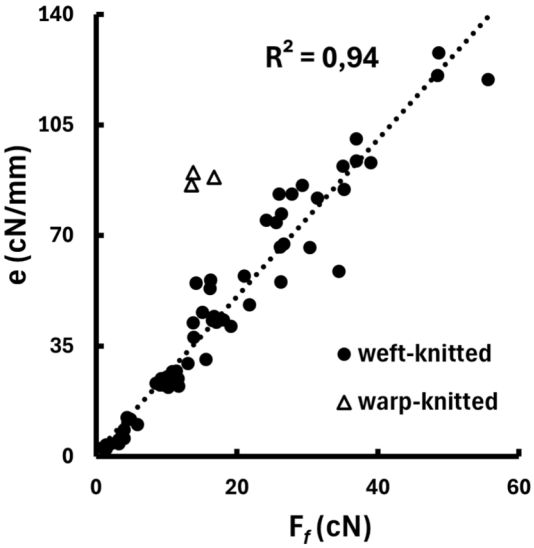

Fig. 21 Stiffness *e* in function of the flattening stress by weft-knitting structures stress by knitting structures

Only 2.1% of the thickness distribution is already compressed at $\delta = \delta_{av}$—2*S*.The flattening can be considered to begin at 2*S* from the average thickness, then the simplification $\delta_{av} = 2S$ is made to obtain a simplified expression of Φ(δ) (Eq. 13). F_f then becomes the integral the compression stiffness from 0 to 3*S* (Eq. 14). It can be observed on the equation that F_f is then the product of *e* and a function of *S*. For *S* constant, F_f and *e* are in a linear relationship. Since S is stable the relationship between F_f and *e* appears almost linear. Using the equation with S = 0.362, the ratio $e / F_f = 2.57$ mm^{-1} was calculated. This value shows only a 3.8% variation from average ratio measured and proves the coherence of the flattening model presented in this article. The force required to flatten a weft-knitted spacer fabric depends almost entirely on the stiffness of its spacer units.

$$\Phi(\delta) = \int_{-\infty}^{\delta} \frac{1}{\sqrt{2\pi S^2}} e^{-\frac{(t-2S)^2}{2S^2}} dt \tag{13}$$

$$F_f = e \times \int_{0}^{3S} \Phi(\delta) d\delta \tag{14}$$

The warp-knitted sample shows a different ratio e / F_f with an average value of 6.30 mm^{-1} and a standard deviation of 0.66 mm^{-1}, the weft-knitted specimens have much lower values with a maximum at only 3.88 mm^{-1}. As for the

weft-knitted spacer fabrics the equations and are used to calculate the ratio $e / F_f = 6.31\ mm^{-1}$ which is very close to the average measured value.

4 Conclusion

For this study a set of 20 weft-knitted spacer fabrics was knitted with a variation of 5 independent knitting parameter: their outer layer yarn, elastic yarn, knitting structure, material and diameter of the spacer yarn. The 20 weft-knitted spacer fabrics and 1 warp-knitted spacer fabric were subjected to a compression test to measure their thickness as well as their flattening and compression properties. A new standard method using an inverse analysis procedure to measure the fabric thickness was developed. The accuracy of the method could prove that the thickness distribution within a fabric follows a normal law and that the different parts of the spacer layer go through independent compressions. A simpler but less precise measurement method using a linear model was also developed, this secondary measurement method often showed a high accuracy but was also proved to produce consequent errors. This new method as well as a current measurement method using a threshold stress value of 1 kPa were used to measure the thickness of the samples. The new standard method proved to be efficient, precise and reproducible for all kind of spacer fabrics, when the 1 kPa threshold method was only efficient for fabrics with Young's modulus ranging from 20 to 50 kPa. This proposed standard thickness definition overall improves the accuracy of standardized thickness measurement and provides a harmonized solution to the current confusion of thickness definitions. The proposed standard thickness was also compered to an ideal thickness value calculated with a geometric model, this model predicted the fabric thickness with a higher accuracy than the fixed threshold stress value, showing only 3.8% variation from the standard thickness on average. This simple model can be extremely useful to estimate a fabric thickness without performing compression test and data analysis. A model to predict the flattening stress of spacer fabrics was developed and showed very high accuracy. This developed model offers a great potential to predict the flattening stress of spacer fabrics. However, further research might be needed to validate the model's performance with warp-knitted fabrics as only one sample was tested.

Acknowledgements The authors Ulysse Le Coz and Pierre Ringenbach received scholarships for PhD candidates, respectively from the National University Corporation Kyoto Institute of Technology Fund and the Otsuka Toshimi Scholarship Foundation.

Author contributions U.L. conceptualized the study, processed the data, developed the models and wrote the original draft. U.L. and P.R. set the experimental design, produced the samples and conducted the mechanical tests. AS set the methodology. A.S and A.Y. supervised the study, they reviewed and edited the manuscript. AY provided the textil materials.

Data availability The data that support the findings of this study have been deposited in a Nomad archive under the name "Spacer flattening datat" at the provided link: https://nomad-lab.eu/prod/v1/gui/search/entries/entry/id/xomJ86u0×1xhgb914mkUkLSee0og.

Declarations

Competing interests The authors declare no competing interests.

References

1. Albaugh L, McCann J, Yao L, Hudson S. Engineering multifunctional spacer fabrics through machine knitting. Conference on Human Factors in Computing Systems, Yokohama, Japan, 8–13 May 2021; https://doi.org/10.1145/3411764.3445564

2. Buzaite V, Mikucioniene D. Effect of inner layer structures of weft-knitted spacer fabrics on thermal insulation and air permeability. Text Res J. 2022. https://doi.org/10.1177/00405175211021452.
3. Klausmann J, Mutschler T, Holderied P, et al. Thermodynamic qualification of knitted spacer fabrics for use as insulation box insert in the context of refrigerated transport containers in the logistics sector. Commun Dev Assem Text Prod. 2023. https://doi.org/10.25367/cdatp.2023.4.p18-26.
4. Wu Q, Hu J. A novel design for a wearable thermoelectric generator based on 3D fabric structure. Smart Mat Struct. 2017. https://doi.org/10.1088/1361-665X/aa5694.
5. Schmidl G, Jia G, Gawlik A, et al. Aluminum-doped zinc oxide–coated 3D spacer fabrics with electroless plated copper contacts for textile thermoelectric generators. Mat Today Energy. 2021. https://doi.org/10.1016/j.mtener.2021.100811.
6. Zheng Y, Zhang Q, Jin W, et al. Carbon nanotube yarn based thermoelectric textiles for harvesting thermal energy and powering electronics. J Mat Chem A. 2020. https://doi.org/10.1039/c9ta12494b.
7. Wang Z, Ruan Z, et al. Integrating a triboelectric nanogenerator and a zinc-ion battery on a designed flexible 3D spacer fabric. Small Method. 2018. https://doi.org/10.1002/smtd.201800150.
8. Li M, Chen J, Zhong W, et al. Large-area, wearable, self-powered pressure-temperature sensor based on 3D thermoelectric spacer fabric. ACS Sens. 2020. https://doi.org/10.1021/acssensors.0c00870.
9. Liu Y, Hu H. Sound absorption behavior of knitted spacer fabrics. Text Res J. 2010. https://doi.org/10.1177/0040517510373639.
10. Mousavi G, Varsei M, Rashidi A, Ghazisaeidi R. Experimental evaluation of the compression garment produced from elastic spacer fabrics through real human limb. J Ind Text. 2022. https://doi.org/10.1177/1528083720988089.
11. Liu Y, Hu H, Zhao L, Long H. Compression behaviour of warp-knitted spacer fabrics for cushioning applications. Text Res J. 2012. https://doi.org/10.1177/0040517511416283.
12. Rajan T, Souza L, Ramakrishnan G, Zakriya G. Comfort properties of functional warp-knitted polyester spacer fabrics for shoe insole applications. J Ind Text. 2016. https://doi.org/10.1177/1528083714557056.
13. Chen S, Zhang X, Chen H, Gao X. An experimental study of the compression properties of polyurethane-based warp-knitted spacer fabric composites. Autex Res J. 2017. https://doi.org/10.1515/aut-2016-0010.
14. Zhao T, Long H, Yang T, Liu Y. Cushioning properties of weft-knitted spacer fabrics. Text Res J. 2018. https://doi.org/10.1177/0040517517705630.
15. Li N, Yick K, Yu A, Ning S. Mechanical and thermal behaviours of weft-knitted spacer fabric structure with inlays for insole applications. Polym. 2022. https://doi.org/10.3390/polym14030619.
16. Li N, Yick K, Yu A. Novel weft-knitted spacer structure with silicone tube and foam inlays for cushioning insoles. J Ind Text. 2022. https://doi.org/10.1177/15280837211073359.
17. Yu A, Sukigara S, Masuda A. Investigation of vibration isolation behaviour of spacer fabrics with elastic inlay. J Text Eng. 2020. https://doi.org/10.4188/jte.66.65.
18. Yu A, Sukigara S, Masuda A. Vibration isolation properties of novel spacer fabric with silicone inlay. Polym. 2023. https://doi.org/10.3390/polym15051089.
19. Yu A, Sukigara S. Investigation of materials for palm and dorsal of anti-vibration gloves for thermal comfort. Fash Text. 2023. https://doi.org/10.1186/s40691-023-00340-0.
20. Chen F, Liu Y, Hu H. An experimental study on vibration isolation performance of weft-knitted spacer fabrics. Text Res J. 2016. https://doi.org/10.1177/0040517515622149.
21. Chen F, Hu H. Nonlinear vibration of knitted spacer fabric under harmonic excitation. J Eng Fiber Fabr. 2020. https://doi.org/10.1177/1558925020983561.
22. Frydrysiak M, Pawliczak Z. Vibro-insulation properties for spacer knitted fabric as a comparative study. J Ind Text. 2021. https://doi.org/10.1177/1528083719888677.
23. Guo Y, Chen L, Qiang S, Qian X, et al. Comparing Properties of the Warp-knitted spacer fabric instead of sponge for automobile seat fabric. J Phys Conf Ser. 2021. https://doi.org/10.1088/1742-6596/1948/1/012196.
24. Karahan M, Gul H, Karahan N, Ivens J. Static behavior of three-dimensional Integrated core sandwich composites subjected to three-point bending. J Reinf Plast Compos. 2013. https://doi.org/10.1177/0731684412474857.
25. Asayesh A, Amini M. The effect of fabric structure on the compression behaviour of weft-knitted spacer fabrics for cushioning applications. J Text Inst. 2021. https://doi.org/10.1080/00405000.2020.1829330.
26. Asayesh A, Amini M. Analysis of the compression performance of weft-knitted spacer fabrics for protective applications in view of the surface layer structure. Fiber Polym. 2021. https://doi.org/10.1007/s12221-021-0248-y.
27. ISO 5084:1997. Determination of thickness of textiles and textile products.
28. JIS L 1096:2010. Testing methods for woven and knitted fabrics.
29. Ertekin G, Marmarali A. The compression characteristic of weft knitted spacer fabrics. Tekst Konfekt. 2012;22:340–5.
30. Wardiningsih W, Rudy R, Permana M, et al. Study of structural parameters of weft knitted spacer fabrics on wound dressing performance. Text Leather Rev. 2024. https://doi.org/10.31881/TLR.2024.057.
31. Rajan P, Prakash C, Ramakrishnan G. An effect of fabrics thickness and structure on moisture management properties of 3D spacer fabrics. Int J Cloth Sci Technol. 2019. https://doi.org/10.1108/IJCST-01-2019-0002.
32. ASTM D1777–96:2019. Standard Test Method for Thickness of Textile Materials 1. https://doi.org/10.1520/D1777-96R19
33. Liu Y, Hu H. Compression property and air permeability of weft-knitted spacer fabrics. J Text Inst. 2011. https://doi.org/10.1080/00405001003771200.
34. Kawabata S. The standardization and analysis of hand evaluation. Textile Machinery Society of Japan; 1980.
35. Parachuru R. The Kawabata evaluation system and its application to product/process enhancement. Beltwide cotton conferences, Atlanta, USA, 8–12 January 2002.
36. Chen C, Du Z, Yu W, Dias T. Analysis of physical properties and structure design of weft-knitted spacer fabric with high porosity. Text Res J. 2018. https://doi.org/10.1177/0040517516676060.
37. Harris DC. Nonlinear least-squares curve fitting with microsoft excel solver. J Chem Educ. 1998. https://doi.org/10.1021/ed075p119.